


Selected Scattering on Quasi-Ordered Hexagonal Close-Packed Al Nanodents for Tunable Output of White LEDs

Junfeng Zhao ^{1,2}, Xinxiang Yu ^{1,2} , Zhiguo Zhao ³, Xiaoyan Dong ¹, Dandan Shi ³, Xianli Shi ³, Jie Sun ¹, Mingfu Zhang ⁴ and Han Dai ^{1,2,4,*}

¹ Laboratory of Advanced Light Alloy Materials and Devices, Yantai Nanshan University, Longkou 265713, China

² Postdoctoral Station of Nanshan Group Co., Ltd., Longkou 265706, China

³ Hang Xin Material Technology Co. Ltd., Longkou 264006, China

⁴ Guizhou University of Engineering Science, Bijie 551700, China

* Correspondence: daihan1985@189.cn; Tel.: +86-0535-859-0938

Received: 2 August 2019; Accepted: 30 August 2019; Published: 3 September 2019



Abstract: Quasi-ordered hexagonal close-packed Al nanodents, with depths of 30 nm and top-diameters of 300 nm prepared by electrochemical anodizing, are used to manage the output spectrum of white Light Emitting Diodes (LEDs). Significant short wavelength light, with a peak of 450 nm, displays significant scattering enhancements on these Al nanodents with the increment of the angle of the incidence, while long wavelength light, with a peak of 550 nm, shows weaker scattering on Al nanodents with the increment of the incidence angle. Near-field and far-field simulations reveal the effect of light coupling in the holes of Al nanodents on the selected scattering. This work could provide a striking new way to make use of cheap white LEDs.

Keywords: Al nanodents; selected light scattering; white LED; nanomaterials

1. Introduction

The invention of high efficiency white Light Emitting Diodes (LEDs) has created a new chapter for the use of energy and lighting [1–3]. As the white LEDs have been widely used in interior lighting, the fact that short wavelength light causes damage to eyes due to the wave crest in the blue band of the LED spectrum, especially the cheap ones, has drawn great attention [4–7]. The common resolution of the wave crest in the blue band of the LED spectrum is through the control of the red, green and blue (RGB) or the use of fluorescent substances to absorb the excessive blue light [8–11]. However, the former way needs expensive electronic devices to achieve the matching of each component of the RGB; the latter method has the output of the white LED fixed, which limits their application ranges.

Recently, the enhanced selected light transmission in the visible spectrum of metal nanostructures such as Ag, Au, Al, and Cu has been designed and widely used in the antireflection layer of solar cells, the transmission-increasing layer in LEDs, and even in the highest possible resolution color filters [12–15]. Furthermore, a cheap way of fabricating large-scale quasi-ordered hexagonal close-packed Al nanodents on Al foil using electrochemical etching has been reported [16,17]. These Al nanodents show optical characteristics similar to those of sub-wavelength grating [18], exhibiting strong near-field enhancement and selected light scattering properties. As a result, the application of Al nanodents has become a new choice for light filters in LED sources.

Herein, quasi-ordered hexagonal close-packed Al nanodents were prepared and used to manage the output spectrum of white LEDs. The selected scattering enhancement of short wavelength light with a peak of 450 nm was found on Al nanodents, with the increment of the incidence angle ranging

from 30° to 70°. However, long wavelength light with a peak of 550 nm was found to show weaker scattering under the same conditions. Meanwhile, slight peak shifts in the output of long wavelength light were observed. The reason why Al nanodents exhibit selected scattering characteristics was clarified by finite difference time domain (FDTD) simulations.

2. Materials and Methods

Following the anodic oxidation process reported [19,20], Al nanodents were prepared by electrochemically anodizing Al foil in a mixture of 0.3 M aqueous solution of oxalic acid and ethanol with a ratio of 1:3 for 3 h at 0 °C. Anodic aluminum oxides were etched out in a mixture of phosphoric acid (6 wt%) and chromic acid (1.8 wt%) at 60 °C for 12 h. Quasi-ordered hexagonal close-packed nanodents were obtained on the Al foils. The thickness of the Al foil was about 0.5 mm, making it completely optically opaque. To show the universality of the selected scattering of Al nanodents, a cheap white LED composed of a blue LED @ with yellow phosphor was used as the lighting source.

Simulations based on FDTD of the near-field light enhancement and the far-field scattering on Al nanodents were performed [21]. In our model, the electromagnetic pulse fixed at 450 and 550 nm for the incidence light (from 0° to 60°) was launched into a box containing the target Al nanodents to simulate a propagating plane wave interacting with the nanostructure. The overlap region of the gold tip was divided into 5 nm meshes. The refractive index of the surrounding medium was taken to be 1.0. The Al nanodents were modeled at 30 nm depth with 300 nm top diameters according to the atomic force microscope (AFM) measurements, the far-field scattering of Al nanodents was prepared, and the scattering light was collected on a hemispherical surface with a diameter of 1 m.

The morphology of Al nanodents was characterized with a field emission scanning electron microscope (SEM, Hitachi UHR FE-SEM SU8010). The depth of the Al nanodents were characterized with an AFM (Agilent 5500) and the far-field scattering light was characterized with an optical fiber spectrometer (Ocean USB 4000).

3. Results and Discussion

As shown in Figure 1a, a white LED source was used to illuminate Al nanodents from different angles in the range of 0° to 70°. The divergence angles of LED sources ranged from 13° to 15°. Through the lens collimation, the divergence angle was reduced to less than 5° in our case. The far-field light output of the LED was collected and characterized by an optical fiber spectrometer, keeping a distance of 2 cm from the sample, as shown in Figure 1a. Similar operations were used to measure the scattering spectra in the opposite direction. The source spectrum is presented in the inset in Figure 1a and shows two typical peaks around 450 and 550 nm. As shown in Figure 1b, Al nanodents exhibit blue scattering across the whole foil under vertical illumination of the white LED source. The morphology of Al nanodents was obtained with SEM and AFM, as shown in Figure 1c,d. The average size of these ordered hexagonal close-packed nanodents was about 300 nm, whereas the depth of the nanodents was relatively shallow, only about 30 nm.

As shown in Figure 2b, strong blue light scattering was found on the surface of the Al nanodents illuminated with white LED. The blue light scattering became stronger with the increment of the incidence angle from 0° to 60°. A simple schematic diagram was used to illustrate the position of the photos taken, as shown in Figure 2a. Obviously, light within the short wavelength range (blue) was first separated when the viewpoint ranged from 0° to 60°. At large angles (>70°), weak light with longer wavelengths (green and yellow) were separated. However, the scattering intensity of light with longer wavelengths was very weak, therefore the scattering of Al nanodents was mainly localized in the short wavelength range.

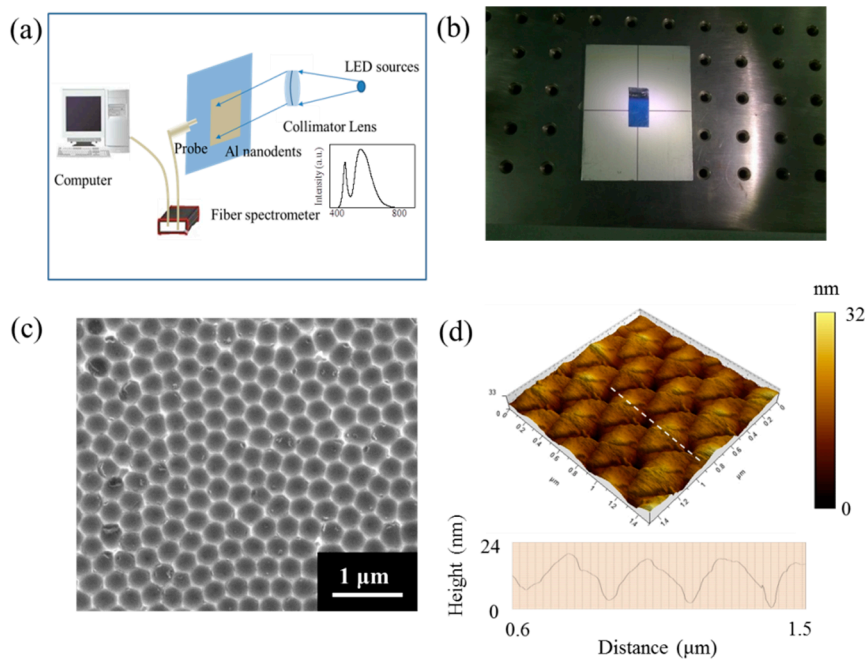


Figure 1. White Light Emitting Diodes (LED) scattering on Al nanodents. (a) A schematic diagram of optical measuring devices including the LED source, collimating lens group, optical fiber spectrometer, and Al nanodents; inset is the spectrum of the light source. (b) Optical image of the Al nanodents lighted by the LED source. (c) SEM image of the quasi-ordered hexagonal close-packed Al nanodents. (d) Depth of the Al nanodents obtained by atomic force microscope (AFM).

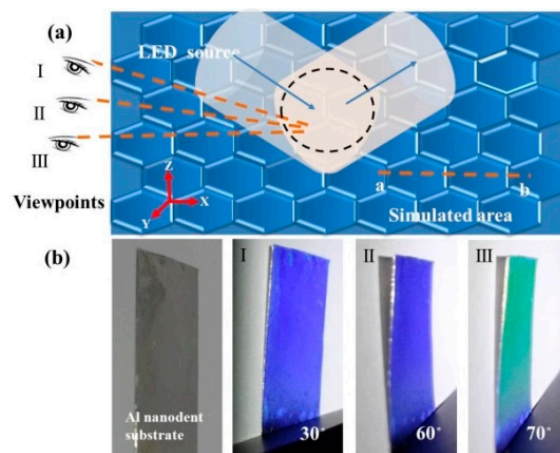


Figure 2. Schematic diagram of the white LED light scattering on Al nanodents. (a) Schematic diagram of the scattering. (b) Image of the Al nanodents with normal illumination and white LED illumination with a 50° incidence angle from 30°, 60°, and 70° viewpoint angles (I, II, and III).

To further understand the selected scattering of Al nanodents, the light scattering spectra and the output spectrum of white LED were characterized simultaneously. The light peak around 450 nm in Figure 3a was found to grow higher as the incidence angle increased from 30° to 70°. In contrast to the light peak around 450 nm, the light peak around 550 nm decreased with the increment of the incidence angle, which confirms the selected scattering in short wavelength ranges on Al nanodents. The spectrum of outputs also proves such selected scattering, as shown in Figure 3b. Significant reduction of the light intensity in the short wavelength range was clearly observed as the incidence angle increased from 30° to 70°. In order to distinguish the peak in 550 nm, we added 0% to 20% (interval 5%) to the value of the intensity of light, with the incidence angle ranging from 30° to 70° in Figure 3b. With the increment of the incidence angle, a few intensity changes were observed at

550 nm and a slight red shifts was observed to occur at the peak of 550 nm. The reason for the red shifts was that at very large incidence angles, the scattering of light with longer wavelengths is enhanced, as shown in Figure 2b. Meanwhile, selective light scattering did result in a reduction of light intensity by about 5–10% in the whole spectrum, which was mainly caused by the back scattering of light within short wavelengths. Through further optical design, combined with the selective coating of specific areas of down-conversion dyes, it is believed that the scattered light with short wavelengths will also be fully utilized. As a result, the ratio of the light component can be simply controlled by changing the angle of incidence. Considering their selected light scattering properties, Al nanodents can be used as simple light filters for cheap white LEDs to reduce the damage caused by blue light.

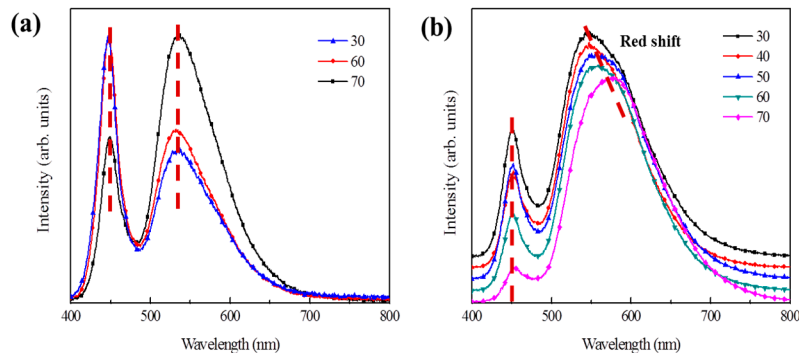


Figure 3. Scattering (incident direction) and output spectrum of the white LED on Al nanodents. (a) Scattering spectrum (incident direction) of the white LED light scattering on Al nanodents. (b) Output spectrum of the white LED light with incidence angles from 30° to 70°.

A far-field model based on FDTD simulation was used on quasi-ordered hexagonal close-packed Al nanodents to prove such angle-dependent selected light scattering, as shown in Figure 4. In this model, the scattering light was collected on a hemispherical surface (diameter of 1 m) with periodic boundary conditions. To better understand the light scattering direction, the direction of the incidence was defined along the Y axis, as shown in Figure 4. The scattered light distribution of the incidence was near the center of the hemispherical surface, presented by polar coordinates. As shown in Figure 4a–c, the scattering of light at a 450 nm wavelength greatly increased with the increment of the incidence angle. The scattering of light was mainly localized along the incident direction, which was along the Y axis. In contrast to light at a 450 nm wavelength, the scattering of light at 550 nm was relatively low, although it grew slightly with the increment of the incidence angle, as shown in Figure 4d–f. Obviously, the far-field simulations coincide well with our experiment observations.

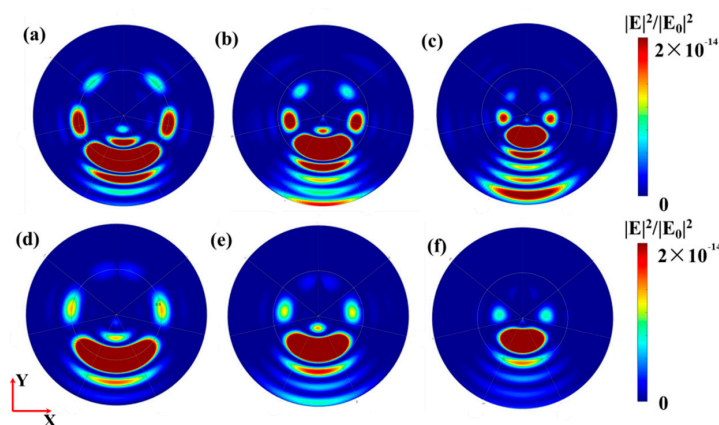


Figure 4. (a–c) Far-field simulations on Al nanodents with 0°, 15°, and 30° incidence angles at a 450 nm wavelength. (d–f) Far-field simulations on Al nanodents with 0°, 15°, and 30° incidence angles at a 550 nm wavelength.

Near-field simulation was also carried out to better understand the selected scattering on Al nanodents. As shown in Figure 5, two light sources were chosen according to the two peaks of the white LED with 450 and 550 nm wavelengths. As shown in Figure 5a–c, no obvious near-field enhancement was found in Al nanodents under vertical incidence (angle of 0°) at both wavelengths of 450 and 550 nm and light was mainly localized in the holes of Al nanodents. Overall, the main difference of the two kinds of light lies in their penetration depth. As shown in Figure 5a–f, the penetration depth of light at the same wavelength increased with the increment of its incidence angle, and the penetration depth of light at a 450 nm wavelength was greater than that at a 550 nm wavelength with the same incidence angle. The selected light scattering of light can be attributed to the interaction between light and holes on the Al nanodents, and only provides efficient light coupling for lights with short wavelengths.

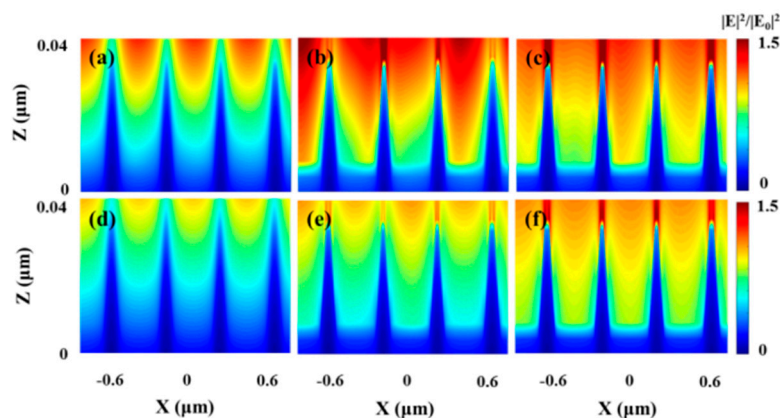


Figure 5. (a–c) Near-field light distribution in Al nanodents with 0° , 15° , and 30° angles of incidence (top to bottom) at a 450 nm wavelength. (d–f) Near-field light distribution with 0° , 15° , and 30° angles of incidence at a 550 nm wavelength.

4. Conclusions

In summary, quasi-ordered hexagonal close-packed Al nanodents have been used to manage the output spectrum of white LEDs. The light scattering on Al nanodents showed high angle- and wavelength-dependence. Through the control of the incidence angle, the intensity of light in white LEDs can be easily tuned. Far-field simulations confirmed the experimental observations. The near-field simulation revealed the relationship between the scattering and the penetration depths of light at different wavelengths on Al nanodents. This work could benefit the application of cheap white LEDs in indoor lighting in less-developed regions.

Author Contributions: Conceptualization, H.D.; Methodology, J.Z.; Software, J.Z.; J.S.; Validation, X.Y.; Formal Analysis, X.D.; Investigation, Z.Z.; Resources, D.S.; Data Curation, J.S.; Writing—Original Draft Preparation, M.Z.; H.D.; Writing—Review and Editing, H.D.; Supervision, X.S.; Project Administration, H.D.; Funding Acquisition, H.D.

Funding: This research was funded by A Project of Shandong Province Higher Educational Science and Technology Program, grant numbers J17KA043, J17KB076, J18KA053; The Natural Science Foundation of Shandong Province, China, grant number ZR2017PEM005; and The Natural Science Research Project of the Guizhou Provincial Education Department, China, grant number KY2015472.

Acknowledgments: This research was supported by Scientific Research Projects of Nanshan Group Co., Ltd.

Conflicts of Interest: The authors declare no conflict of interest.

References

1. Nakamura, S.; Fasol, G. *The Blue Laser Diode*; Springer: Berlin/Heidelberg, Germany, 1997.
2. Yang, Q.; Li, G.; Wei, Y.; Chai, H. Synthesis and photoluminescence properties of red-emitting NaLaMgWO₆: Sm³⁺, Eu³⁺ phosphors for white LED applications. *J. Lumin.* **2018**, *199*, 323–330. [[CrossRef](#)]

3. Pimputkar, S.; Speck, J.S.; DenBaars, S.P.; Nakamura, S. Prospects for LED lighting. *Nat. Photonics* **2009**, *3*, 180–182. [[CrossRef](#)]
4. Oh, J.H.; Yoo, H.; Park, H.K.; Do, Y.R. Analysis of circadian properties and healthy levels of blue light from smartphones at night. *Sci. Rep.* **2015**, *5*, 11325. [[CrossRef](#)] [[PubMed](#)]
5. Wurtman, R.J. Effects of light on human body. *Sci. Am.* **1975**, *233*, 68–77. [[CrossRef](#)]
6. Cajochen, C.Z.; Munch, M.; Kobialka, S.; Krauchi, K.; Steiner, R.; Oelhafen, P.; Orgül, S.; Wirz-Justice, A. High sensitivity of human melatonin, alertness, thermoregulation, and heart rate to short wavelength light. *J. Clin. Endocr. Metab.* **2005**, *90*, 1311–1316. [[CrossRef](#)] [[PubMed](#)]
7. Peng, M.L.; Tsai, C.Y.; Chien, C.L.; Hsiao, J.C.J.; Huang, S.Y.; Lee, C.J.; Yin, L.H.; Cheng, W.Y.; Tseng, K.W. The influence of low-powered family LED lighting on eyes in mice experimental model. *Life Sci. J.* **2012**, *9*, 477–482.
8. Cossu, G.; Khalid, A.M.; Choudhury, P.; Corsini, R.; Ciaramella, E. 3.4 Gbit/s visible optical wireless transmission based on RGB LED. *Opt. Express* **2012**, *20*, B501–B506. [[CrossRef](#)]
9. Uchida, Y.; Taguchi, T. Lighting theory and luminous characteristics of white light-emitting diodes. *Opt. Eng.* **2005**, *44*, 124003. [[CrossRef](#)]
10. Liang, K.; Li, W.; Ren, H.R.; Liu, X.L.; Wang, W.J.; Yang, R.; Han, D.J. Color measurement for RGB white LEDs in solid-state lighting using a BDJ photodetector. *Displays* **2009**, *30*, 107–113. [[CrossRef](#)]
11. Xie, R.J.; Hirotsaki, N.; Takeda, T. Wide color gamut backlight for liquid crystal displays using three-band phosphor-converted white light-emitting diodes. *Appl. Phys. Express* **2009**, *2*, 022401. [[CrossRef](#)]
12. Dai, H.; Zhao, J.; Huang, T.; Yu, X.; Sun, J.; Fang, H.; Zhu, Z.; Yu, K. Plasmonic conglomeration of ultrathin Ag nanofilms far below their melting points by infrared illumination. *Appl. Sci.* **2018**, *8*, 897. [[CrossRef](#)]
13. Lyon, L.A.; Musick, M.D.; Natan, M.J. Colloidal Au-enhanced surface plasmon resonance immunosensing. *Anal. Chem.* **1998**, *70*, 5177–5183. [[CrossRef](#)] [[PubMed](#)]
14. Aryasetiawan, F.; Hedin, L.; Karlsson, K. Multiple plasmon satellites in Na and Al spectral functions from ab initio cumulant expansion. *Phys. Rev. Lett.* **1996**, *77*, 2268. [[CrossRef](#)] [[PubMed](#)]
15. Santos, I.P.; Iglesias, A.S.; González, B.R.; Marzán, L.M.L. Aerobic synthesis of Cu nanoplates with intense plasmon resonances. *Small* **2009**, *5*, 440–443. [[CrossRef](#)] [[PubMed](#)]
16. Huang, H.; Lu, L.; Wang, J.; Yang, J.; Leung, S.F.; Wang, Y.; Chen, D.; Chen, X.Y.; Shen, G.Z.; Li, D.D.; et al. Performance enhancement of thin-film amorphous silicon solar cells with low cost nanodent plasmonic substrates. *Energy Environ. Sci.* **2013**, *6*, 2965–2971. [[CrossRef](#)]
17. Zhang, X.; Wei, X.; Ducker, W. Formation of nanodents by deposition of nanodroplets at the polymer-liquid interface. *Langmuir* **2010**, *26*, 4776–4781. [[CrossRef](#)] [[PubMed](#)]
18. Yang, Z.L.; Li, Q.H.; Ren, B.; Tian, Z.Q. Tunable SERS from aluminium nanohole arrays in the ultraviolet region. *Chem. Commun.* **2011**, *47*, 3909–3911. [[CrossRef](#)] [[PubMed](#)]
19. Masuda, H.; Asoh, H.; Watanabe, M.; Nishio, K.; Nakao, M.; Tamamura, T. Square and triangular nanohole array architectures in anodic alumina. *Adv. Mater.* **2001**, *13*, 189–192. [[CrossRef](#)]
20. Yuan, J.H.; He, F.Y.; Sun, D.C.; Xia, X.H. A simple method for preparation of through-hole porous anodic alumina membrane. *Chem. Mater.* **2004**, *16*, 1841–1844. [[CrossRef](#)]
21. Collino, F.; Fouquet, T.; Joly, P. Conservative space-time mesh refinement methods for the FDTD solution of Maxwell's equations. *J. Comput. Phys.* **2006**, *211*, 9–35. [[CrossRef](#)]

